

Effect of Location in a Cylinder Wake on Dynamics of a Flexible Energy Harvesting Plate

Open
Access

Mohammad Rasidi Rasani^{1,*}, Ahmad Kamal Ariffin¹, Musa Bashir², Jin Wang²

¹ Centre for Integrated Design for Advanced Mechanical Systems (PRISMA), Faculty of Engineering and Built Environment, Universiti Kebangsaan Malaysia, 43600 Bangi, Selangor, Malaysia

² Liverpool Logistics, Offshore and Marine (LOOM) Research Institute, School of Engineering, Technology and Maritime Operations, Liverpool John Moores University, Liverpool L3 3AF, United Kingdom

ARTICLE INFO

ABSTRACT

Article history:

Received 19 July 2017

Received in revised form 29 October 2018

Accepted 6 December 2018

Available online 18 March 2019

Flexible plate in the wake of a bluff body may be exploited to harvest energy, for example by attaching piezoelectric sheets on both surfaces of the plate. A computational investigation on flow-induced vibration of a flexible plate in the wake of a cylinder is undertaken to understand the effects of plate location on their vibrations and hence, energy harvesting potential. Based on cylinder diameter D (0.1m), flow at a sub-critical Reynolds number of 10000 was considered in the present study. The fluid-structure interaction was implemented via a closely-coupled partitioned scheme that employs a Scale-Adaptive Simulation (SAS) of the Shear Stress Transport (SST) method to model flow turbulence. A flexible plate was placed at several locations (streamwise: $x/D = 0.5, 1.0, 1.5, 2.0$; crossflow: $y/D = 0, 0.25, 0.5$) downstream of the cylinder and their flow-induced response were compiled and analysed. Benchmarking of present model showed good agreement with previous experimental investigations. Results suggest that maximum deflection may be found if flexible plate is placed in the region between cylinder surface and $x/D < 1.0$. Oscillation of flexible plate placed at $y/D = 0.25$ shows similar amplitude, if not slightly higher, than if plate is placed at wake centerline. Present findings suggest that energy output may be optimised by positioning flexible energy harvesting plates at favourable locations in the wake region.

Keywords:

Vortex-Induced Vibration, Scale-Adaptive Simulation (SAS), Energy Harvesting

Copyright © 2019 PENERBIT AKADEMIA BARU - All rights reserved

1. Introduction

Depleting fuel supply and issues with global energy security is a major concern worldwide including to the European Union [1]. This has prompted intensive efforts in developing and utilizing renewable and sustainable energy technologies, for example solar energy, wind and ocean energy [2]. One of the many interesting technologies that has been proposed to generate clean and sustainable energy is by exploiting bluff bodies to harvest energy.

Bluff bodies such as cylinders are commonly found in many offshore structures (for example, marine risers, tensioners, pipelines and platform jackets). Beyond a certain Reynolds number, flow

* Corresponding author.

E-mail address: rasidi@ukm.edu.my (Mohammad Rasidi Rasani)

around these cylindrical structures are accompanied by vortex shedding that may lead to lift fluctuation on these cylinders, inducing their vibration and eventual fatigue. As a result, in-situ and automated monitoring of health and safety of these structures have become increasingly important, especially in extended offshore field operations and unpredictable ocean environments [3]. A potential low maintenance, low-cost, clean and portable auxiliary power supply to these monitoring instruments and loggers may be extracted by harvesting energy from the shed vortices or wakes behind these cylindrical structures.

One of a number of concepts to harvest these vortex energy is to place flexible membranes or plates in the wake region downstream of a bluff body [4-8]. These flexible membranes or plates are either made or installed with piezoelectric materials to convert oscillating motion of these membranes as it follows the undulating wake flow, into electrical energy. Apart from harvesting energy, this concept is also potentially attractive as assembling flexible plates behind a cylindrical structure may also be exploited to influence cylinder vortex shedding (see previous studies for example, Wu *et al.*, [9], Shukla *et al.*, [10], Qiu *et al.*, [11] and Lee and You [12]) and thus, minimizing cylinder vortex-induced vibration (VIV) and its corresponding structural fatigue.

Either for harvesting energy or modulating vortex shedding in cylinders, limited attention has been given to the effect of flexible plate location in the wake region, to the dynamics of the flexible plate, which may influence both the amount of energy harvested and the fluctuating forces applied on a cylinder. Therefore, in the present study, we aim to undertake a computational investigation on the effect of flexible plate location behind a cylinder towards the vibration of the plate, and hence their energy harvesting potential. To that end, we simulate unsteady flow around a fixed cylinder interacting with a flexible plate positioned in various streamwise and crossflow positions behind the cylinder. A sub-critical flow around a cylinder at Reynolds number (Re) of 10000 is considered in the present work. As the boundary layer remains laminar but wake region is turbulent, the present computation considers a recently developed Scale-Resolving or Scale Adaptive Simulation (SAS) [13,14] of the Shear Stress Transport (SST) model in the fluid solver, which is capable of predicting more realistic turbulence flowfield compared to conventional URANS turbulence models. The present methodology is validated with a benchmark flow around cylinder and a flexible splitter plate case presented by De Nayer *et al.*, [15].

Details of the methodology and computational model of the present work are described in section 2, followed by validation study of the benchmark case in section 3. Vibration results of the flexible plate at the various positions are compiled and discussed in section 4, followed by concluding remarks in section 5.

2. Methodology

2.1 Flow Equations

Although periodic vortex shedding behind a circular cylinder may begin at around $Re = 50$, previous vortex-induced energy harvesting concepts operate at higher Reynolds numbers, as indicated in Table 1. As a result, a Re of 10000 is considered in this work.

At this Re , flow around cylinder falls in the sub-critical flow regime where flow close to the cylinder surface remains laminar prior to separation but becomes turbulent in the wake region. Therefore, in order to simulate this flow, we considered an Unsteady Reynolds Average Navier-Stokes (URANS) approach using a $k-\omega$ Shear Stress Transport (SST) turbulence model, but with a relatively recent Scale-Adaptive Simulation (SAS) modification proposed by Menter and Egorov [13,14]. Details on the SAS and SST methodology are published previously (see for example, Menter and Egorov [13, 14] and Jadidi *et al.*, [19]) and therefore, only a very brief summary is presented here.

Table 1
 Re operating range of some vortex-induced flexible plate vibration energy harvesting concept

Case	Re
Allen and Smits [4]	5000 - 40000
Yu and Liu [6]	10600 - 21300
Weinstein <i>et al.</i> , [16]	3000 – 8000
Nguyen <i>et al.</i> , [17]	6024
Shi <i>et al.</i> , [18]	3200 - 12000

The governing URANS equations include conservation of momentum and continuity equations, which may be expressed respectively as Eq. (1) and Eq. (2) below [19].

$$\frac{\partial \bar{u}_i}{\partial t} + \frac{\partial}{\partial x_j} (\bar{u}_i \bar{u}_j) = -\frac{1}{\rho} \frac{\partial \bar{p}}{\partial x_i} + \frac{\partial}{\partial x_j} \left[(\nu + \nu_t) \left(\frac{\partial \bar{u}_i}{\partial x_j} \right) \right] \quad (1)$$

$$\frac{\partial \bar{u}_i}{\partial x_i} = 0 \quad (2)$$

where \bar{u}_i and \bar{p} are the time-averaged fluid velocities and pressures respectively ($i, j = 1, 2, 3$ represent the 3-D cartesian directions), ρ denotes fluid density and ν represents the fluid kinematic viscosity. ν_t is the turbulent eddy viscosity, which for SST model, is estimated based on turbulence kinetic energy (k) and specific dissipation rate (ω) equations.

Although conventional SST models has a number of advantages (see for example, [20]), similar to other URANS models, it may overpredict turbulence length scales and eddy viscosities. Instead, an SAS treatment in the SST model estimates a von Kármán length-scale and introduces a corresponding source term into the specific dissipation rate (ω) equation, allowing the model to switch to LES-like simulations [14,19]. Therefore, more unsteady turbulent structures are resolved as mesh is refined, but at more reasonable computational costs.

2.2 Structural Equations

Time-dependant deformation of a structure follows the conservation of momentum equation [21]:

$$\rho \ddot{\mathbf{d}} = \nabla \cdot \sigma_{ij} + \mathbf{f} - c \dot{\mathbf{d}} \quad (3)$$

where σ_{ij} is the stress tensor and the first term on the right-hand side accounts for stiffness and elastic modulus of structure. In addition, c represents damping ratio, ρ denotes density of structure material, \mathbf{d} represents displacements of structure and \mathbf{f} represents a time-dependent external force acting on structure. In the present work, we considered neglecting structural damping.

2.3 Computational Model

Figure 1 illustrates the computational domain employed, where dimensions in the streamwise (x) \times crossflow (y) \times spanwise (z) directions are $25D \times 12D \times 1D$ (D denoting diameter of cylinder). The stationary circular cylinder is placed $5D$ downstream of the inlet boundary, $20D$ away from the outlet boundary and is symmetrically $6D$ away from top and bottom boundaries. With the present fluid-structure interaction problem, the computational domain consists of domain for both fluid (i.e. flow domain surrounding the cylinder and flexible plate) and structure (i.e. flexible plate).

Although at $Re = 10000$ flow around cylinder becomes three dimensional, we explored a 2-D simulation in the present study (with a $1D$ span width) as the computational benefit may be advantageous considering the reasonable accuracy achieved in predicting fluid forces (as shown in previous 2-D studies, for example in Derakhshandeh *et al.*, [22] and Rajani *et al.*, [23]). Corresponding boundary conditions for the flow domain is summarised in Figure 1, where both right and left faces of the domain are prescribed as symmetric conditions and the stationary cylinder surface are prescribed as no-slip walls. For the structural domain, the flexible plate is cantilevered where its leading edge is fixed.

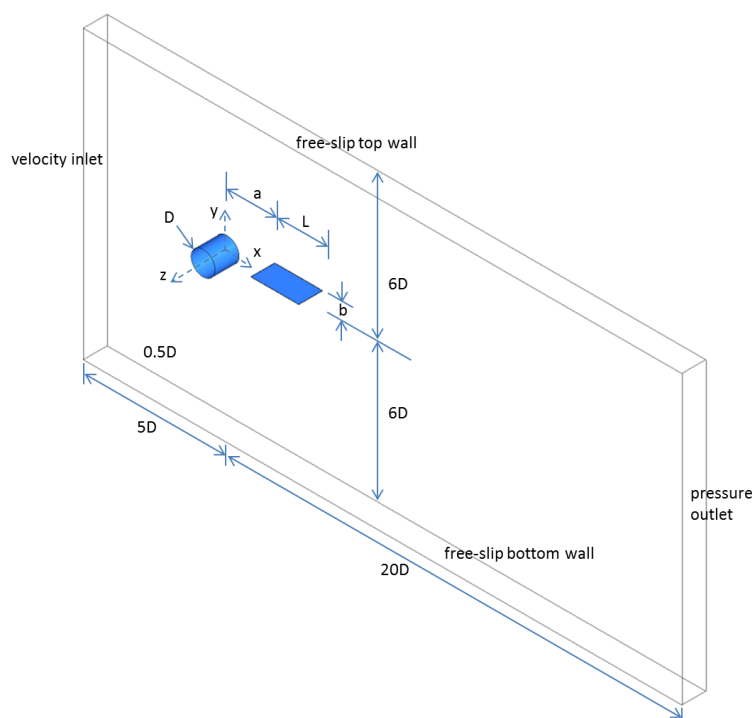


Fig. 1. Computational domain and boundary conditions

Tables 2, 3 and 4 compiles the relevant geometry, flow and structural parameters respectively in the present study.

Table 2
 Geometrical parameters in present study

Cylinder diameter, D	100 mm	
Plate length, L	200 mm	$L/D = 2$
Plate thickness, h	0.8 mm	
Plate x -location, a	$x/D = 0.5, 1.0, 1.5, 2.0$	
Plate y -location, b	$y/D = 0, 0.25, 0.5$	

For idealizing an energy harvesting flexible plate, we considered an elastic rubber plate (elastic modulus $E = 16$ MPa, poisson ratio $\nu = 0.48$) sandwiched between two $110 \mu\text{m}$ thick piezoelectric sheets ($E = 1000$ MPa, $\nu = 0.34$), leading to composite properties shown in Table 4.

Table 3

Flow parameters for the present study

Inlet velocity, U_∞	1.545 m/s
Outlet pressure	1 atm.
Fluid density, ρ	1.185 kg/m ³
Fluid dynamic viscosity, μ	1.831×10^{-5} Pa s
Reynolds Number (based on diameter), Re_D	10000

Table 4

Structural parameters for flexible plate

Material density, ρ	1780 kg/m ³
Elastic modulus, E	286.9 MPa
Poisson ratio, ν	0.346

Unstructured grids were employed to discretise the non-uniform flow computational domain, with denser grid points closer to the cylinder and flexible plate surfaces, as shown in Figure 2. Spacing of the first grid point normal to the cylinder and flexible plate surface is prescribed as $0.001D$, keeping maximum dimensionless wall distance $y^+ < 2$ in all cases. In total, the baseline grid consist of 13544-15886 unstructured grids (depending on case) for the flow domain and 466 structured grids for the flexible plate.

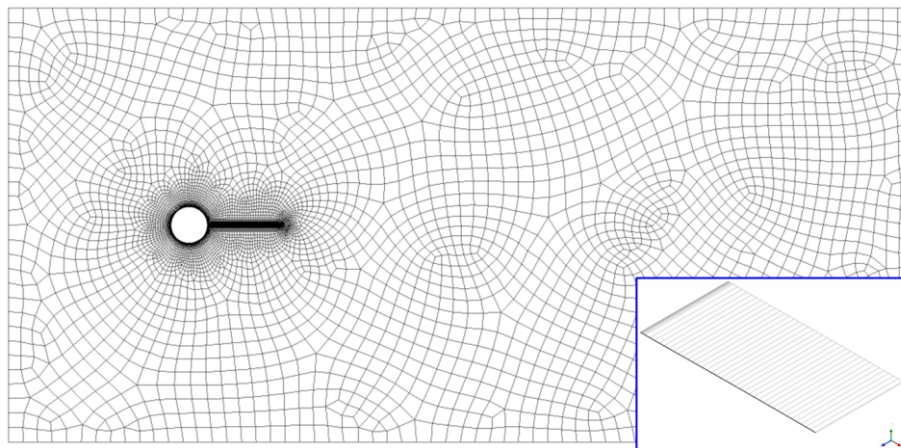


Fig. 2. Grids used for the flow and structure (inset) computational domain

A total of 12 cases were simulated, corresponding to total combinations of streamwise (x) and crossflow (y) locations considered for flexible plate placement (i.e. a and b shown in Figure 1 and Table 2). Coupling between the fluid and structural solver was implemented using a partitioned approach, where an Arbitrary Lagrangian Eulerian framework is used in the fluid solver to account for grid movement as the fluid grids adapt to the interfacing structure movement. All unsteady fluid-structure interaction simulations were initiated from the steady-state solution of a stationary plate condition. A coupling under-relaxation factor of 0.5 and 0.75 were considered respectively for displacements and load transfer, to closely couple the fluid-structure iterations at each timestep. The governing flow equations were solved using a second order backward euler scheme for time

advancement, where timestep size were chosen such that maximum CFL (Courant-Friedrichs-Lewy) number was kept in the order of $O(1)$. Considering transients in the initial fluid-structure interactions, statistical results were obtained by time-averaging results beyond non-dimensional time $tU_\infty/D = 100$. All the flow and structural modelling were implemented respectively using a computational fluid dynamic and finite element solver, which were coupled inside an ANSYS Workbench Release 17 platform [24].

3. Preliminary Studies

We begin by comparing results from the present modelling with previous benchmark cases in order to verify the approach in the present study.

3.1 Stationary Plate Behind Cylinder

In this case, the solution for a case where plate is located at $x/D = 0.5$, $y/D = 0$ and is initially stationary, is compared to a well-known experiment on wake splitter plate by Apelt *et al.*, [25]. Table 5 presents results of present model in comparison with previous benchmark investigations. For $L/D = 2$ and $Re = 10000$, present model predicts a cylinder drag coefficient (C_d) of 0.89 in comparison to corresponding experimental measurement of 0.93 [25].

Table 5
Comparisons with benchmark cases at $Re_D = 10000$

Case	Stationary	Flexible	
	\bar{C}_d	u_y/D	St
Experiments [25]	0.93		
Experiments [15]		0.5	0.16
Present model	0.89	0.42	0.15

3.2 Flexible Plate Behind Cylinder

The present model is used to simulate water flow around a smaller cylinder ($D = 22$ mm) and smaller flexible plate ($L = 60$ mm, $h = 2$ mm) made of pure rubber, following a recent experimental and numerical study for FSI benchmarking by De Nayer *et al.*, [15]. Since the added mass effect is more pronounced as water is displaced following the flexible plate movement, a closer partitioned coupling is necessary in this case, resulting in increased number of internal coupling iterations per timestep. At $Re = 10000$, the maximum vertical displacement (u_y) of flexible plate tip and Strouhal number (St) predicted in the present model is in reasonable agreement with experimental measurements, as summarised in Table 5.

To summarise, result of C_d from the present model compares well to the benchmark result of a stationary plate behind a cylinder experiment [25], indicating that the number of grids and meshing distribution used in the present model is sufficient to predict accurate flow separation. In addition, the present model also show agreement with a well-established benchmark experiment of a flexible plate behind a cylinder [15], suggesting that the number of grids employed in both fluid and structural models are justified to capture appropriate flow behaviour and structural response, even though the fluid grids are deforming and moving dynamically with the oscillating flexible plate.

4. Results and Discussion

In order to assess the effect of flexible plate placement inside the wake region on plate vibration and considering symmetry about wake centerline, 12 cases were simulated. Each case corresponds to different locations in the wake region where flexible plate is positioned. Figure 3 shows the 12 positions where leading edge of flexible plate is fixed and their corresponding case numbers labelled. On average, 10-20 internal coupling iterations were required for fluid-structure convergence at each timestep, and simulations may run up to 14 hours on certain cases.

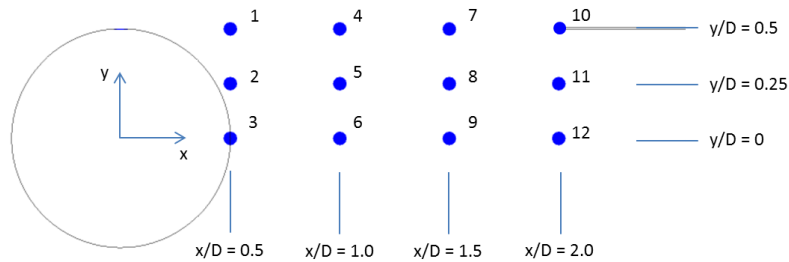


Fig. 3. Locations for placement of flexible plate leading edge (highlighted by dots) and corresponding case numbers (labelled 1-12)

Figure 4 depicts a representative contour of instantaneous spanwise vorticity and flexible plate vibration mode obtained in the present study. Vibration of flexible plate appears closer to its first bending mode motion in all cases simulated, which is perhaps consistent with the low sub-critical Re of present study. In addition, unlike plate located along wake centerline, vortex shedding from cylinder is not symmetrical when plate is positioned at $y/D = 0.25$.

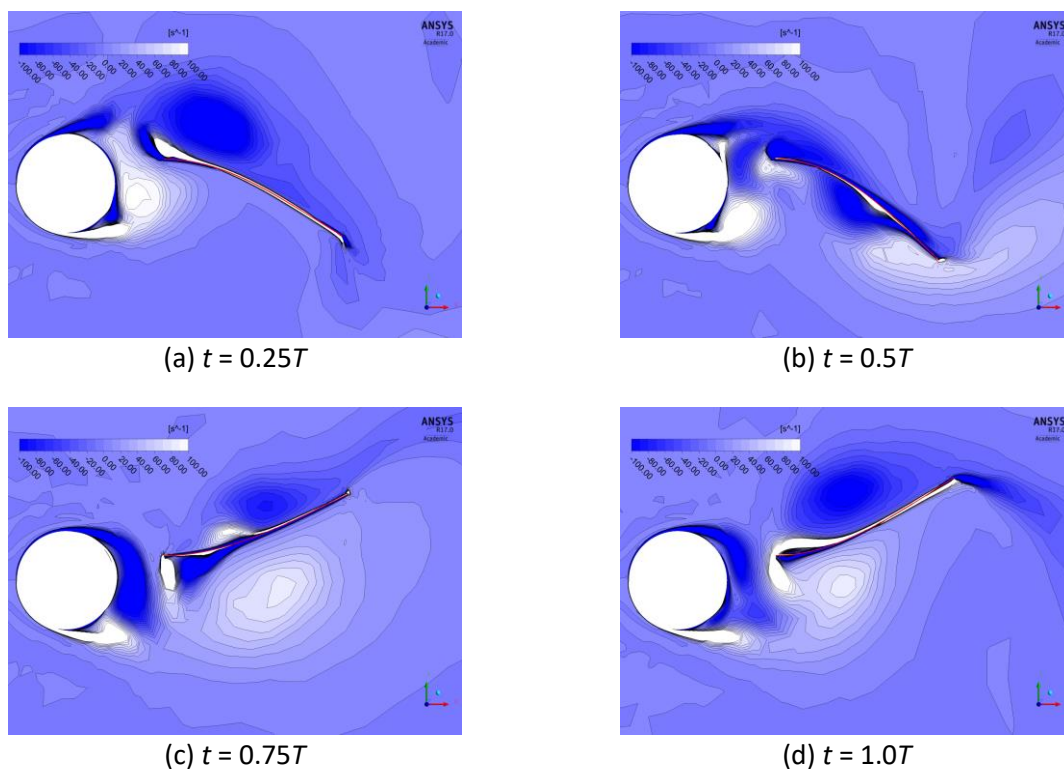


Fig. 4. Plot of instantaneous spanwise vorticity contours and motion of flexible plate (highlighted in red) for case 5 (T indicates one period of plate oscillation)

Figure 5 presents the y-deflection of the flexible plate trailing edge tip, showing that oscillation amplitude reduces as flexible plate is placed further downstream from the cylinder, which may be explained by streamwise reduction in vortex strength as indicated in Figure 4. However, maximum oscillating amplitude is not located at $x/D = 0.5$ close to the cylinder, but instead at $x/D = 1.0$. Furthermore, although placing flexible plates at centerline ($y/D = 0$) of wake region shows high amplitudes are sustained farther downstream, oscillation for plate located at $y/D = 0.25$ indicates similar, if not higher, amplitudes. This may suggest that a favourable location for increased oscillation (and hence, increased energy harvesting output) may potentially be found at a region between $0.5 < x/D < 1.0$ and $0 < y/D < 0.25$.

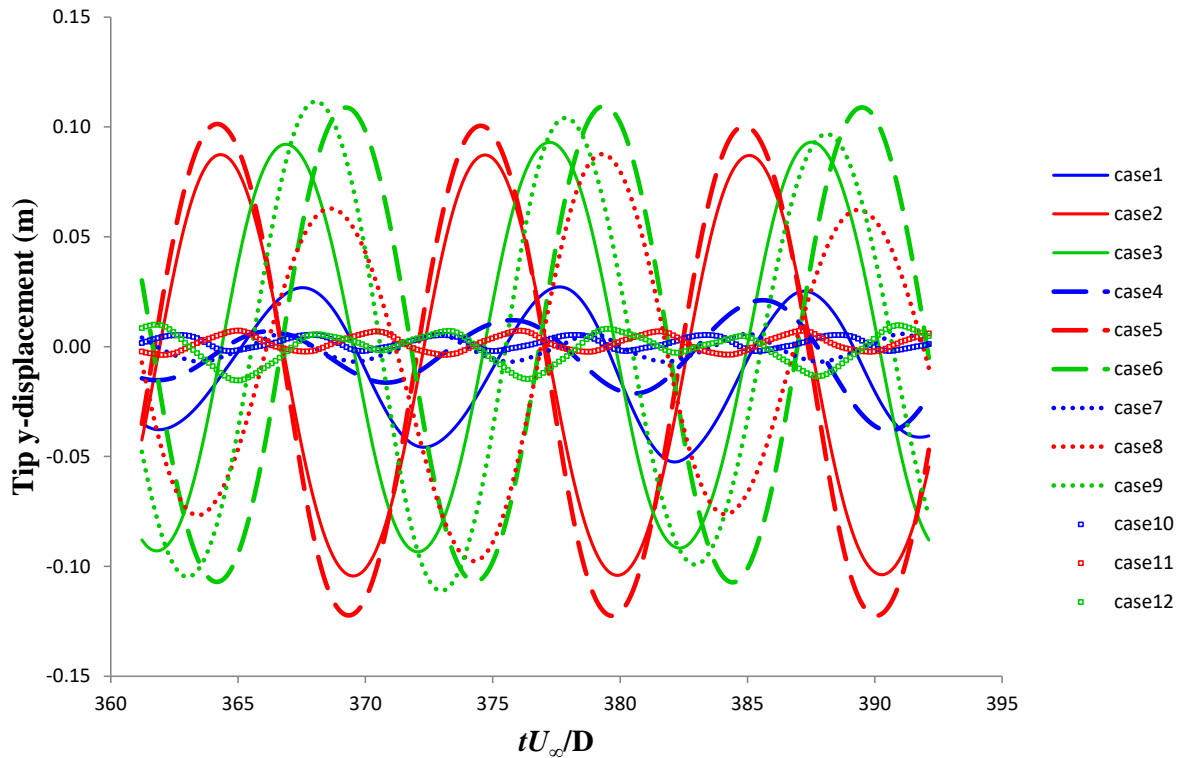


Fig. 5. Plot of tip deflection against non-dimensional time for all cases: solid lines for cases at $x/D = 0.5$, dashed lines for cases at $x/D = 1.0$, dotted lines for cases at $x/D = 1.5$ and squared markers for cases at $x/D = 2.0$

Oscillation amplitudes of plate tip when flexible plate is placed at various locations in the cylinder wake region, are summarised in Figure 6. Flexible plate positioned at $y/D = 0.5$ shows low amplitude of oscillations, at all streamwise locations. In addition, amplitude of oscillation is higher for plates located at $y/D = 0.25$ compared to centerline-located plate, for streamwise locations $x/D \leq 1$, but is lower for streamwise locations $x/D > 1$.

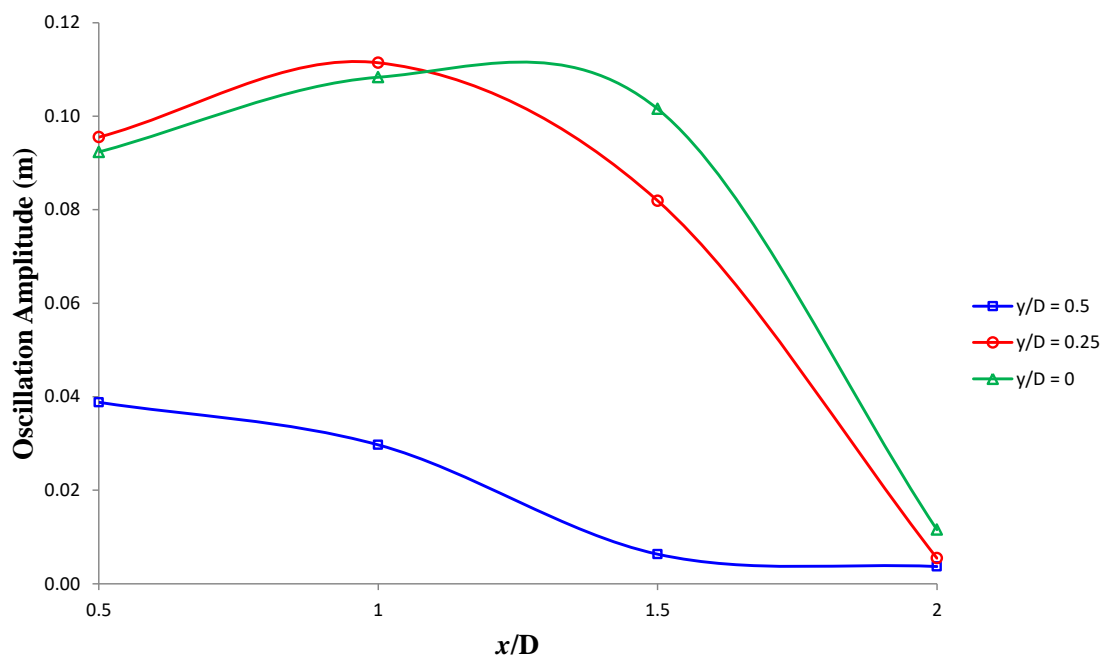


Fig. 6. Plot of tip oscillation amplitude against placement of flexible plate

5. Conclusions

Flow-induced vibration of a flexible plate in the wake of a circular cylinder at $Re_D = 10000$ was numerically investigated using a Scale-Adaptive Shear Stress Transport model, in order to identify effect of flexible plate placements inside the wake on their vibrations. Comparison of the present model with benchmark cases at $Re_D = 10000$, showed good agreement with previously published experimental results. A series of simulation cases at different locations in the wake were undertaken at the considered Re_D , indicating that amplitude of plate oscillation may be maximised at a region slightly downstream from the cylinder. This suggest that flexible plate energy harvesting may be optimised by placing them at favourable locations in the cylinder wake. Future studies on the effect of Re_D on flexible plate dynamics in the wake and further experimental work are intended.

Acknowledgement

This work is supported by EU H2020 Marie Curie RISE project no. 730888 (RESET). All types of support from Liverpool John Moores University and Universiti Kebangsaan Malaysia are gratefully acknowledged.

References

- [1] Khattak, M.A., M.A.H Ayoub, M.A.F. Abdul Manaf, M.F. Mahrul, M.R. Mohd Juhari, M.I. Mustaffa, S. Kazi. "Global energy security and European Union: A review." *Journal of Advanced Research in Applied Sciences and Engineering Technology* 11 (2018): 64-81.
- [2] Zuan, A.M.S., M.K.Z. Anuar, S. Syahrullail, M.N. Musa, E.A. Rahim. "A study of float wave energy converter (FWEC) model." *Journal of Advanced Research in Applied Sciences and Engineering Technology* 1 (2015): 40-49.
- [3] Mukundan, Harish, Yahya Modarres-Sadeghi, Jason Michael Dahl, Franz S. Hover, and Michael S. Triantafyllou. "Monitoring VIV fatigue damage on marine risers." *Journal of Fluids and structures* 25, no. 4 (2009): 617-628.
- [4] Allen, J. J., and A. J. Smits. "Energy harvesting eel." *Journal of fluids and structures* 15, no. 3-4 (2001): 629-640.
- [5] Taylor, George W., Joseph R. Burns, S. A. Kammann, William B. Powers, and Thomas R. Welsh. "The energy harvesting eel: a small subsurface ocean/river power generator." *IEEE journal of oceanic engineering* 26, no. 4 (2001): 539-547.

- [6] Yu, Yuelong, and Yingzheng Liu. "Flapping dynamics of a piezoelectric membrane behind a circular cylinder." *Journal of Fluids and Structures* 55 (2015): 347-363.
- [7] Bhuyan, M. S., Burhanuddin Yeop Majlis, Masuri Othman, Sawal H. Md Ali, C. Kalaivani, and S. Islam. "Bluff body fluid interactions modelling for micro energy harvesting application." In *Journal of Physics: Conference Series*, vol. 431, no. 1, p. 012024. IOP Publishing, 2013.
- [8] Akaydin, H. D., Niell Elvin, and Yiannis Andreopoulos. "Wake of a cylinder: a paradigm for energy harvesting with piezoelectric materials." *Experiments in Fluids* 49, no. 1 (2010): 291-304..
- [9] Wu, J., C. Shu, and N. Zhao. "Numerical study of flow control via the interaction between a circular cylinder and a flexible plate." *Journal of Fluids and Structures* 49 (2014): 594-613.
- [10] Shukla, S., R. N. Govardhan, and J. H. Arakeri. "Dynamics of a flexible splitter plate in the wake of a circular cylinder." *Journal of Fluids and Structures* 41 (2013): 127-134.
- [11] Qiu, Y., Y. Sun, Y. Wu, and Y. Tamura. "Effects of splitter plates and Reynolds number on the aerodynamic loads acting on a circular cylinder." *Journal of Wind Engineering and Industrial Aerodynamics* 127 (2014): 40-50.
- [12] Lee, Jinmo, and Donghyun You. "Study of vortex-shedding-induced vibration of a flexible splitter plate behind a cylinder." *Physics of Fluids* 25, no. 11 (2013): 110811.
- [13] Menter, Florian, and Yury Egorov. "A scale adaptive simulation model using two-equation models." In *43rd AIAA aerospace sciences meeting and exhibit*, p. 1095. 2005.
- [14] Menter, F. R., and Y. Egorov. "The scale-adaptive simulation method for unsteady turbulent flow predictions. Part 1: theory and model description." *Flow, Turbulence and Combustion* 85, no. 1 (2010): 113-138.
- [15] De Nayer, Guillaume, Andreas Kalmbach, Michael Breuer, Stefan Sicklinger, and Roland Wüchner. "Flow past a cylinder with a flexible splitter plate: A complementary experimental–numerical investigation and a new FSI test case (FSI-PfS-1a)." *Computers & Fluids* 99 (2014): 18-43.
- [16] Weinstein, Lee A., Martin R. Cacan, P. M. So, and P. K. Wright. "Vortex shedding induced energy harvesting from piezoelectric materials in heating, ventilation and air conditioning flows." *Smart Materials and Structures* 21, no. 4 (2012): 045003.
- [17] Nguyen, Hai-Dang Tam, Huy-Tuan Pham, and Dung-An Wang. "A miniature pneumatic energy generator using Karman vortex street." *Journal of Wind Engineering and Industrial Aerodynamics* 116 (2013): 40-48.
- [18] Shi, Shengxian, T. H. New, and Yingzheng Liu. "Flapping dynamics of a low aspect-ratio energy-harvesting membrane immersed in a square cylinder wake." *Experimental Thermal and Fluid Science* 46 (2013): 151-161.
- [19] Jadidi, Mohammad, Farzad Bazdidi-Tehrani, and Mohsen Kiamansouri. "Scale-adaptive simulation of unsteady flow and dispersion around a model building: spectral and POD analyses." *Journal of Building Performance Simulation* 11, no. 2 (2018): 241-260.
- [20] Jehad, D. G., G. A. Hashim, A. K. Zarzoor, and CS Nor Azwadi. "Numerical Study of Turbulent Flow over Backward-Facing Step with Different Turbulence Models." *Journal of Advanced Research Design* 4, no. 1 (2015): 20-27.
- [21] Xia, Guohua, and Ching-Long Lin. "An unstructured finite volume approach for structural dynamics in response to fluid motions." *Computers & structures* 86, no. 7-8 (2008): 684-701.
- [22] Derakhshandeh, Javad Farrokhi, Maziar Arjomandi, Bassam Dally, and Benjamin Cazzolato. "The effect of arrangement of two circular cylinders on the maximum efficiency of Vortex-Induced Vibration power using a Scale-Adaptive Simulation model." *Journal of Fluids and Structures* 49 (2014): 654-666.
- [23] Rajani, B. N., A. Kandasamy, and Sekhar Majumdar. "On the reliability of eddy viscosity based turbulence models in predicting turbulent flow past a circular cylinder using URANS approach." *Journal of Applied Fluid Mechanics* 5, no. 11 (2012): 67-79.
- [24] ANSYS, C. "ANSYS CFX-Solver Theory Guide, Vol. Release 17.0, 2016."
- [25] Apelt, C. J., G. S. West, and Albin A. Szewczyk. "The effects of wake splitter plates on the flow past a circular cylinder in the range $10 < R < 5 \times 10^4$." *Journal of Fluid Mechanics* 61, no. 1 (1973): 187-198.